AIAA JOURNAL
Vol. 44, No. 3, March 2006

Effect of Quenching Kinetics on Unsteady Response of Pressure-Sensitive Paint

James W. Gregory* and John P. Sullivan†
Purdue University, West Lafayette, Indiana 47907-2023

Pressure-sensitive paints (PSP) have recently been extended to high-frequency flowfields. Paint formulations have been used effectively to characterize pressure fluctuations on the order of 100 kHz. As the limits of PSP are extended, various experimental results indicate that the unsteady response characteristics are nonlinear. A thorough understanding of the photophysical mechanisms in paint response is needed. Gas transport properties, coupled with the nonlinear nature of the Stern–Volmer relationship have an effect on the paint response. This work discusses the full implications of a diffusion-based model for the unsteady response of pressure-sensitive paint. Based on this model, it is shown that the indicated pressure response of PSP is faster for a decrease in pressure, and slower for a pressure increase. Effects of other factors, such as pressure-jump magnitude, pressure-jump range, and Stern–Volmer nonlinearity, are evaluated. Furthermore, a fluidic oscillator is used to demonstrate experimentally the quenching kinetics of two types of PSP—polymer/ceramic and fast FIB. Results from the oscillator operated with argon, nitrogen, and oxygen gases at 1.59 kHz demonstrate behavior that agrees with the diffusion model. The polymer/ceramic PSP exhibited no delay between different test gases, indicating a flat frequency response of at least 1.59 kHz. Fast FIB, on the other hand, demonstrated a significant delay in rise time between the nitrogen and oxygen cases. Both the diffusion model and the experimental results demonstrate that the different responses to nitrogen and oxygen only become critical when the period of the flowfield oscillations is shorter than the response time of the paint formulation.

Nomenclature

A, B, K	=	Stern–Volmer calibration constants
C	=	gas concentration
C_0	=	reference gas concentration
D_m	=	diffusion coefficient, μm^2/s
$f(t)$	=	time history of gas concentration at the paint surface
$g(t')$	=	normalized form of f
$g_t(t')$	=	first derivative of g with respect to time
h	=	paint thickness, μm
I	=	paint intensity
$\bar{I}$	=	intensity per unit thickness
I_{ref}	=	paint intensity at a reference condition
I_0	=	paint intensity in the absence of oxygen
N	=	number of samples in a time-history
n	=	nondimensional gas concentration
$[O_2]$	=	oxygen concentration
P	=	pressure, Pa
P'	=	nondimensional pressure
P_{ref}	=	reference pressure, Pa
Q	=	heat of adsorption, J/mol
R	=	universal gas constant, 8.31447 J/mol · K
T	=	temperature, K
t	=	time, s
t'	=	nondimensional time, tD_m/h^2
u	=	substituted time variable
$W(t, z)$	=	solution of the diffusion equation
z	=	paint thickness coordinate measured from paint surface, μm
z'	=	nondimensional thickness, z/h
α	=	modal states
γ	=	exponent for the Freundlich isotherm
λ	=	eigenvalues
τ	=	time constant, s
τ_{ads}	=	adsorption time, s
τ_0	=	oscillation time of molecules in the adsorbed state, 1.6×10^{-13} s
$\bar{\phi}$	=	average phase delay
ω	=	frequency, Hz

Presented as Paper 2004-0879 at the AIAA 42nd Aerospace Sciences Meeting, Reno, NV, 5–8 January 2004; received 15 December 2004; revision received 13 May 2005; accepted for publication 27 August 2005.

*Ph.D. Fellow, School of Aeronautics and Astronautics, 315 N. Grant Street; jim.gregory@alumni.purdue.edu. Student Member AIAA.

†Professor, School of Aeronautics and Astronautics, 315 N. Grant Street. Senior Member AIAA.

Introduction

PRESSURE-SENSITIVE paint (PSP) has recently emerged as a powerful measurement tool for global pressure distributions.[1–3] PSP is an optical method for measuring surface pressures based on the oxygen quenching of a luminescent molecule. Reviews by Bell et al.[4] and Liu et al.[5] have summarized the PSP technique and common applications. Furthermore, Liu and Sullivan have written a recently published book that details the development and application of luminescent paints.[6]

Typical paints are composed of an oxygen-sensitive molecule known as the luminophore and a physical binder or matrix for the luminophore. Because luminophores are available with very short lifetimes (∼1 μs), the binder typically limits the frequency response of the paint. Traditional polymer binders have response times as long as seconds. The recent emergence of porous binders, however, has enabled measurements of unsteady pressure fluctuations on the order of 100 kHz. Development of binders for unsteady measurements has generally focused on improving the oxygen diffusivity within the binder. Common binders in use today for unsteady measurements are thin-layer chromatography plate,[7] anodized aluminum,[8–11] polymer/ceramic,[12,13] poly[1-(trimethylsilyl)-1-propyne] (polyTMSP),[14–16] and fast FIB (fluoro/isopropyl/butyl).[17] Thin-layer chromatography plate is commonly used in chemistry laboratories and is composed of a thin layer (∼250 μm) of silica gel. The disadvantages of the thin-layer chromatography plate are that it is fragile and limited to simple shapes. Anodized aluminum is created through an electrochemical process by etching small pores (∼10-nm diameter) on an aluminum surface. The luminophore is deposited directly on the porous surface by chemical and physical

adsorption. Anodized aluminum is regarded as providing the fastest PSP response times, but is limited by the choice of material and cannot be sprayed onto a model. Polymer/ceramic PSP is a hybrid that uses a small amount of polymer with a large amount of ceramic particles. The resulting aggregate is a highly porous surface that allows for rapid diffusion. The primary advantage of polymer/ceramic PSP is that it may be sprayed on a model, and offers reasonable response times. Poly(TMSP) is a functional polymer with extremely high oxygen permeability. Its response is much faster than most polymer binders, but still quite a bit slower than the new porous PSP formulations. FIB is a fluorinated copolymer originally developed at the University of Washington as an "ideal" paint. Fast FIB, essentially a thin layer of FIB, has recently been developed by Innovative Scientific Solutions, Inc., for unsteady measurements.

Dynamic calibrations with a shock tube[10] and a fluidic oscillator[18,19] have shown that most porous PSP formulations have typical frequency responses in excess of 10 kHz. Anodized aluminum PSP has been further developed and characterized by Kameda et al.[20] such that the reported response time is less than 10 μs. Unsteady pressure fields such as the fluidic oscillator (22 kHz),[19,21,22] a turbocharger compressor (10 kHz),[22,23] or the oscillating shock in a Hartmann tube (12 kHz)[24] have been characterized. Some of these experimental results[22] apparently indicate that the dynamic response of PSP is nonlinear. These results have suggested that the response to an increase in oxygen concentration may be slower than the response to a corresponding increase in nitrogen concentration.

The purpose of this paper is to develop a model for the quenching dynamics of pressure-sensitive paint. The implications of the model on the dynamic response of PSP are discussed in detail. Furthermore, it will be shown that the diffusion-based model is applicable to the recently developed fast PSP formulations. Experimental results from the fluidic oscillator will illustrate the effects of the quenching dynamics and will be compared with the theoretical model.

Background

Polymer chemists have done a large amount of experimental and theoretical work on the quenching kinetics of luminescent molecules immobilized in a polymer binder. It has been known for quite some time that the luminescent response of a luminophore in a polymer matrix is different for oxygen sorption or desorption experiments. Chemists have used these observations along with simple diffusion models to determine the diffusivity of a polymer film. The first known published work involving this method was by MacCallum and Rudkin.[25] These researchers applied a simplified form of this model to the measurement of the oxygen diffusion coefficient in two polymer films. Cox and Dunn[26] also measured the oxygen diffusion coefficient via temporal fluorescence quenching in a polymer. The films used by Cox and Dunn were 1 cm thick, resulting in response times on the order of hours. They also demonstrated excellent agreement between the diffusion model and experimental results. Carraway et al.[27] discussed the kinetics of quenching due to several possible models, including pure diffusion, adsorption, and other combinations of models. Perhaps the clearest explanation of the diffusion model and its interaction with the Stern–Volmer relation is given by Mills and Chang.[28] Subsequent researchers[29–35] have used the diffusion modeling technique extensively and report a fast luminescent response to oxygen sorption and a slower response to oxygen desorption.

Within the field of PSP research, there has been some work done to model and experimentally determine the dynamic response characteristics of pressure-sensitive paints. Liu et al.[36] developed a phenomenological model describing the time constant for paint response. They showed that the traditional square-law estimate for paint response,

$$\tau \propto h^2/D_m \tag{1}$$

is valid only for traditional polymer binders. Liu et al. derived a modified relation,

$$\tau \propto h^{2-d_{\mathrm{fr}}}/D_m \tag{2}$$

for highly porous surfaces, where d_{fr} is the fractal dimension that represents the complexity of the pore pathway. Furthermore, Liu et al. invoked the Fickian diffusion model, lending credence to the current use of a diffusion model with porous paints. Kameda et al.[20] discuss gaseous transport in relation to the porous structure of anodized aluminum PSP. They suggest that the diffusion model is valid for anodized aluminum paints, but with a modified diffusion coefficient. Since the Knudsen number for molecular motion within the porous structure is on the order of 1, Kameda et al. posited that a modified diffusion coefficient is necessary because of Knudsen diffusion. This effective diffusion coefficient varied with the pore diameter over a range from 10 to 100 nm, and with pressure. Schairer[37] also employed a diffusion model in his analysis of optimum thickness of a PSP layer, which he found to be a tradeoff between signal-to-noise ratio and dynamic response. Carroll et al.[38] modeled the PSP step response with a diffusion-based model and compared the response times of three different polymer-based PSP formulations. Winslow et al.[39] developed both an empirical model as well as a physics-based diffusion model, with the aim of developing a compensator. They applied both a linear calibration and a Stern–Volmer calibration to the diffusion model and showed that the Stern–Volmer calibration provides a better fit to the experimental data. Winslow et al. also briefly compared the predicted step response behavior of the Stern–Volmer model to the linear model. Most recently, Drouillard and Linne[40] applied the diffusion-based model to luminescent lifetime measurements with PSP. They incorporated Beer's law into their model to account for attenuation of light in a paint layer that is not optically thin. When compared to experimental results, however, optical thickness only appeared to be a relevant parameter at paint thicknesses greater than 45 μm. Drouillard and Linne also quoted a value of mass diffusivity for Uni-FIB paint of somewhere between 300 and 1000 μm^2/s.

Although these models have shown the basic behavior of the quenching kinetics of PSP, an exhaustive evaluation of the PSP dynamics is needed. The effects of factors such as the pressure-jump magnitude, the range over which the jump occurs, and the direction of the pressure jump need to be evaluated. This work demonstrates that not only the paint thickness and diffusion coefficient, but also the expected pressure range, mean pressure, and calibration coefficients, are important factors in determining whether a PSP formulation is suitable for a dynamic test.

Stern–Volmer Quenching Model

Model Development

PSP quenching kinetics may be modeled by the one-dimensional diffusion equation, as others have done in the past.[6,36–39] The following development is a summary of the model, after the derivation of Liu and Sullivan.[6] The response of the PSP may be modeled by considering the diffusion of a test gas into or out of the binder. It is assumed that the diffusion process, rather than the much faster luminophore quenching process, controls the paint response characteristics. If the paint layer is thin and uniform, the gas diffusion is assumed to be one-dimensional and Fickian,[41] expressed as

$$\frac{\partial C}{\partial t} = D_m \frac{\partial^2 C}{\partial z^2} \tag{3}$$

where z is distance measured from the paint surface, as shown in Fig. 1. Fickian diffusion also assumes that there is no mass convection present in the flow. In addition, the time scales of adsorption effects are assumed to be negligible relative to the diffusion and unsteady pressure timescales. The effects of adsorption will be discussed in detail in a later section. The boundary conditions for the diffusion equation are

$$\frac{\partial C}{\partial z} = 0 \quad \text{at} \quad z = h, \qquad C = C_0 f(t) \quad \text{at} \quad z = 0 \tag{4}$$

where $f(t)$ is a function that describes the time history of gas concentration at the paint surface. The initial state of the paint layer

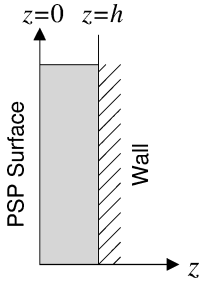

Fig. 1 Diagram of modeled PSP geometry.

is a uniform gas concentration throughout the thickness. Thus, the initial condition for the diffusion equation (3) is

$$C = C_0 f(0) \qquad \text{at} \qquad t = 0 \tag{5}$$

To make the diffusion equation tractable for numerical solution, the following nondimensional variables are introduced:

$$n(t', z') = C/C_0 - f(0), \qquad z' = z/h, \qquad t' = tD_m/h^2 \tag{6}$$

The diffusion equation may then be rewritten as

$$\frac{\partial n}{\partial t'} = \frac{\partial^2 n}{\partial z'^2} \tag{7}$$

with boundary and initial conditions

$$\frac{\partial n}{\partial z'} = 0 \qquad \text{at} \qquad z' = 1, \qquad n = g(t') \qquad \text{at} \qquad z' = 0$$

$$n = 0 \qquad \text{at} \qquad t' = 0 \tag{8}$$

A function $g(t') = f(t') - f(0)$ is used to satisfy the boundary condition at the paint surface. This nondimensional differential equation (7) is then solved with Laplace transforms. When the boundary and initial conditions (8) are applied, a general convolution solution is obtained for the nondimensional gas concentration:

$$n(t', z') = \int_0^{t'} g_t(t' - u) W(u, z')\, \mathrm{d}u \tag{9}$$

The function $g_t(t)$ is the derivative $\partial g(t)/\partial t$, and $W(t, z)$ is defined as

$$W(t, z) = \sum_{k=0}^{\infty} (-1)^k \operatorname{erfc}\left(\frac{1 + 2k - z}{2\sqrt{t}}\right) + \sum_{k=0}^{\infty} (-1)^k \operatorname{erfc}\left(\frac{1 + 2k + z}{2\sqrt{t}}\right) \tag{10}$$

For a step increase in gas concentration at the paint surface, the function g_t is defined as the delta function, $g_t(t) = \delta(t)$, which gives

$$n(t', z') = W(t', z') \tag{11}$$

from the convolution integral (9). Analogously, a step decrease in gas concentration is given by

$$n(t', z') = -W(t', z') \tag{12}$$

From Eqs. (11) and (12), it can be seen that there is no difference in the time scale of diffusion, whether a gas is diffusing into or out of the paint binder. Gas concentration profiles for several time steps of diffusion into and out of the paint binder are shown in Fig. 2. Each step in dimensionless time is given as a successive power of 10 according to

$$t' = 10^{N/4} \qquad \text{where} \qquad -20 \le N \le 2 \tag{13}$$

This diffusion process is independent of the particular gas species of interest. PSP, however, is sensitive only to oxygen concentration. Thus, oxygen diffusion will be the focus of the remainder of this discussion. The sensitivity of PSP to oxygen is dictated by Stern–Volmer quenching behavior, which is an inherently nonlinear relationship.[42] The key to the difference in time scales of the PSP response is in the characteristic nonlinearity of the Stern–Volmer calibration curve. The Stern–Volmer relation may be expressed as[42]

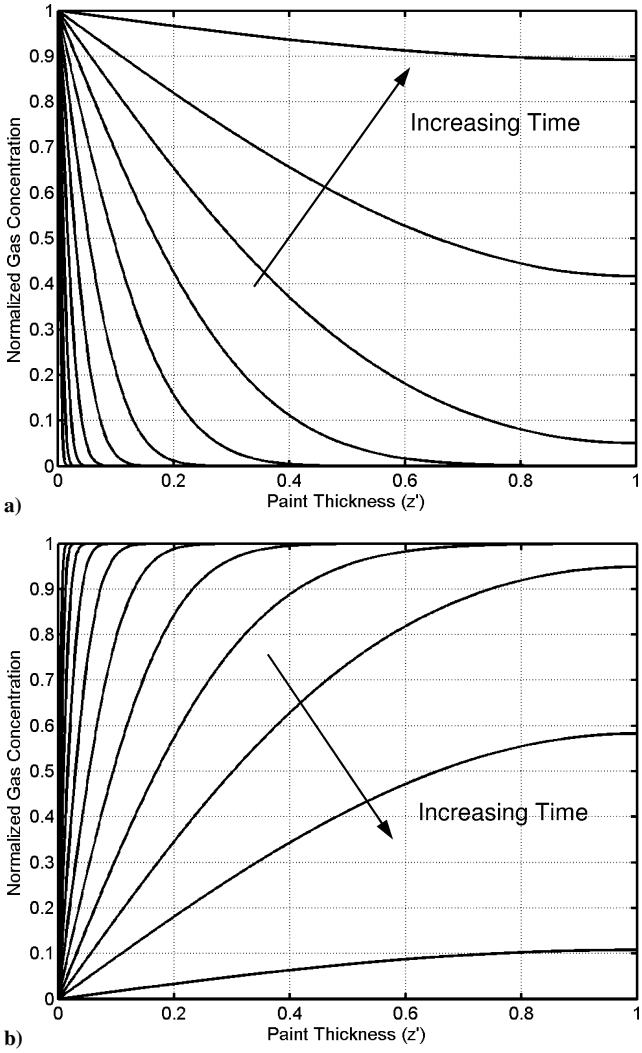

Fig. 2 Gas diffusion a) into and b) out of the paint layer.

$$I/I_0 = 1/(1 + K[\mathrm{O_2}]) \tag{14}$$

where K is a constant if temperature is invariant.

The form of the Stern–Volmer equation typically used for PSP calibrations, given as

$$I_{\mathrm{ref}}/I = A(P/P_{\mathrm{ref}}) + B \tag{15}$$

is obtained by taking the ratio of Eq. (14) under two conditions—a reference and a test condition. When Eq. (14) is compared with the Stern–Volmer form used for PSP calibrations (15), the value of K can be derived as

$$K = A/(B \cdot P_{\mathrm{ref}}) \tag{16}$$

because the concentration of oxygen in air is proportional to the air pressure. A variant of Eq. (15) is the Stern–Volmer relation following the Freundlich isotherm, namely

$$I_{\mathrm{ref}}/I = A(P/P_{\mathrm{ref}})^{\gamma} + B \tag{17}$$

This calibration behavior is characteristic of porous PSP formulations, particularly anodized aluminum PSP. Typical PSP calibration

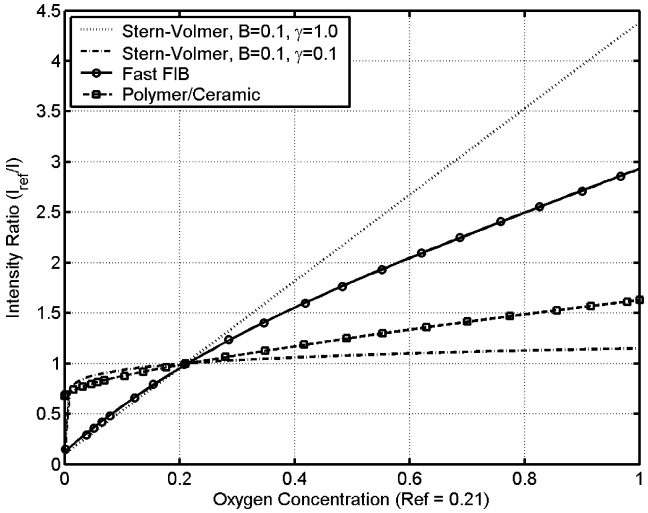

Fig. 3 Typical calibration curves for various PSP formulations.

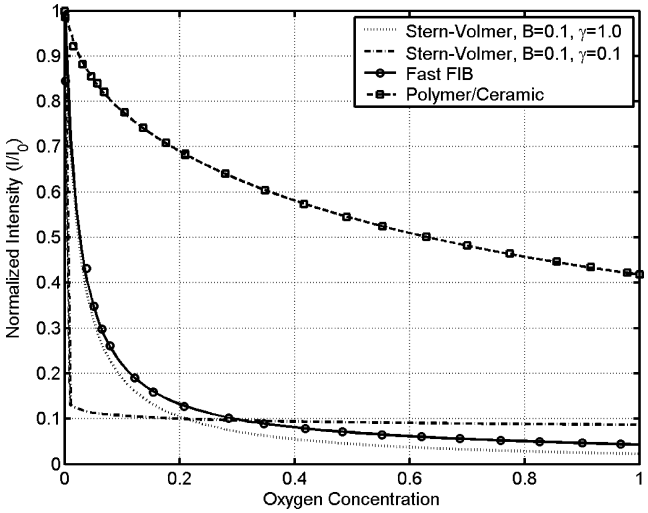

Fig. 4 PSP calibration data plotted to show the nonlinear Stern–Volmer intensity response.

curves for $\gamma = 1.0$ and $\gamma = 0.1$ are shown in Fig. 3, with $A = 0.9$ and $B = 0.1$. In addition to these typical calibration curves, experimental calibrations for the fast FIB and polymer/ceramic formulations are shown in the same figure. PSP calibration data are most often presented as intensity ratio vs pressure ratio, as shown in Fig. 3. This format, however, does not intuitively indicate the nonlinear nature of the Stern–Volmer relationship of Eq. (14). Therefore, the same calibration data are shown in Fig. 4, but with normalized intensity shown (I/I_0) rather than intensity ratio (I_{ref}/I). The highly nonlinear nature of the Stern–Volmer relationship is more readily apparent in this representation. The coupling of the nonlinear intensity response with the diffusion of gas within the paint thickness is the primary mechanism for the difference in rise and fall times of the paint response.

For a given time after the step change in oxygen concentration, there will be a distribution of oxygen within the binder, governed by diffusion relation (3). Therefore, there will also be a variation in paint luminescence within the thickness of the PSP binder, depending on the local oxygen concentration. In the current diffusion-based model, an elemental intensity contribution throughout the paint thickness is determined from the local oxygen concentration. This is determined by the Stern–Volmer relationship, which models the physics of the luminophore intensity response to oxygen concentration. Assuming an optically thin paint layer and a uniform distribution of luminophore in the binder, the luminescent intensity

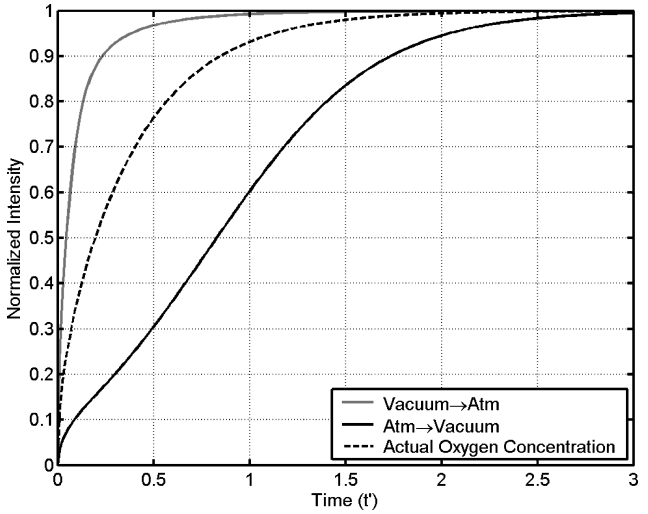

Fig. 5 Integrated intensity response to step changes in pressure compared to oxygen concentration: $A = 0.9$, $B = 0.1$, and $\gamma = 1.0$.

can then be integrated over the thickness of the paint:

$$I(t) = \int_0^h \bar{I}(t, z)\, \mathrm{d}z \tag{18}$$

to give the total luminescent intensity of the paint as a function of time.

Intensity Response

To discretize and solve the diffusion equations, a total of 1000 time steps were used. In addition, the paint thickness was divided into 1000 elemental areas. The summation in Eq. (10) was carried out to 10 terms. These parameters are sufficient to ensure convergence of the solution and are greater than the values used by Winslow et al.[39]

The first case to be considered is a step change in pressure from atmospheric conditions down to vacuum, and back again. The intensity responses for the step increase and step decrease are shown in Fig. 5, along with the shape of the integrated oxygen concentration time history. The intensity profiles have been normalized by

$$I' = \frac{I - I_{\text{initial}}}{I_{\text{final}} - I_{\text{initial}}} \tag{19}$$

to facilitate comparison of waveform shapes. The integrated intensity response to an increase in pressure is much faster than the response to a decrease in pressure. If the Stern–Volmer relationship between intensity and oxygen was linear, then the intensity response for the rise and fall would both collapse to the oxygen concentration curve. Because the Stern–Volmer relation is not linear, the rise and fall responses differ.

Pressure Response

The final step in the simulation is to convert integrated paint intensity back to indicated pressure. This replicates the experimental procedure of acquiring paint intensity data and calibrating the intensity ratio to an indicated pressure ratio. To summarize, the key steps in the modeling procedure are detailed as follows. First, a step change in pressure is modeled at the paint surface. Oxygen concentration throughout the paint thickness is calculated by the diffusion equation for each time step. The resulting temporal and spatial distribution of oxygen is converted to intensity by the Stern–Volmer relationship. The local intensity across the entire paint thickness is then integrated to simulate the experimentally observed intensity for each time step. This integrated intensity is finally converted back to an indicated gas concentration (pressure) by again applying the Stern–Volmer relationship. The result of the model simulation is the paint's indicated response to an arbitrary step change in pressure.

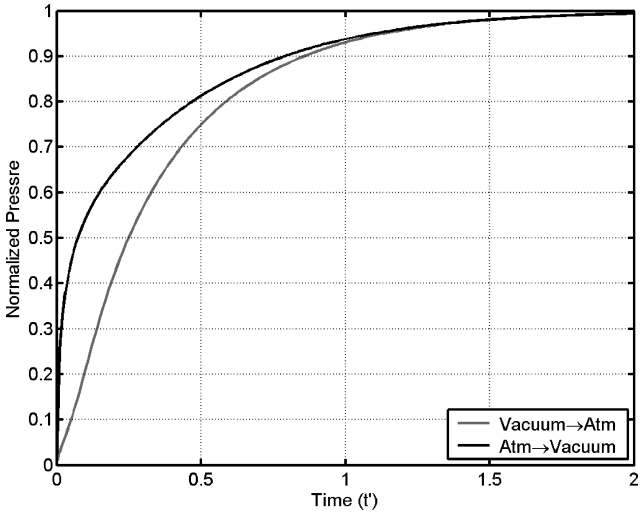

Fig. 6 PSP-indicated pressure step response, variation from atmosphere to vacuum: $A = 0.9$, $B = 0.1$, and $\gamma = 1.0$.

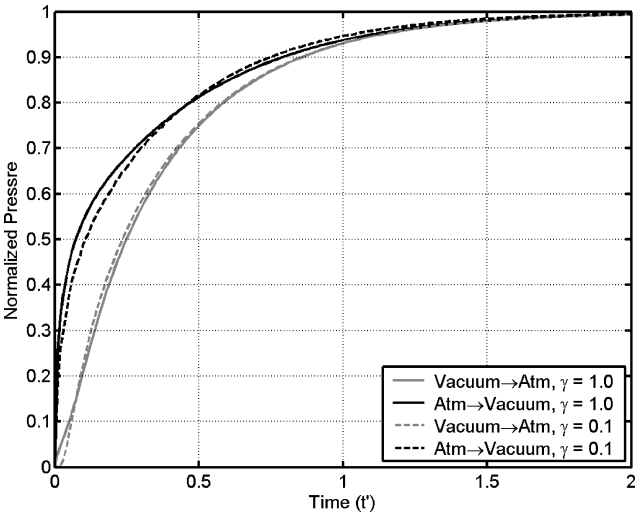

Fig. 7 PSP-indicated pressure step response, variation with γ: $A = 0.9$, $B = 0.1$, and $\gamma = 1.0$ or 0.1.

When the intensity time histories shown in Fig. 5 are converted to pressure, the shapes of the curves change so that the indicated pressure response to a decrease in pressure leads that of an increase in pressure. This result is shown in Fig. 6 for the same parameters used in the solution represented in Fig. 5. The pressure step-response curves have been normalized by

$$P' = \frac{P - P_{\text{initial}}}{P_{\text{final}} - P_{\text{initial}}} \tag{20}$$

in a manner similar to the intensity step-response curves. The change in behavior (contrasted with the intensity profiles) is due to the inversion process within the Stern–Volmer relation. This result also highlights the importance of calibrating experimental intensity results before drawing conclusions about the temporal response characteristics of PSP. For both modeling and experimental work (even flow visualization), the observed time history may be altered significantly if the intensity is not calibrated to pressure or gas concentration.

The pressure response curves in Fig. 6 are plotted against nondimensional time:

$$t' = t/\tau = tD_m/h^2 \tag{21}$$

Note the effects that the paint thickness (h) and diffusion coefficient (D_m) have on the step response of the paint. A thinner paint sample will have a much faster response time. Likewise, a paint binder with a high diffusion coefficient will also exhibit a faster response time. Thus, the relative impact of the response differences to a step increase or step decrease will depend on the diffusion coefficient and thickness of the paint sample being implemented.

The effect of γ in the Freundlich isotherm calibration (17) on the PSP response is also evaluated. Figure 7 shows the results with $A = 0.9$, $B = 0.1$, and $\gamma = 1.0$ or 0.1. The Freundlich isotherm does have some effect on the shape of the indicated pressure–time history, although the effect is minimal. The basic trend remains the same: there is a fast response to a step decrease and a slower response to a step increase in pressure.

The effects of a small change in pressure are shown in Fig. 8. For this case, a change in pressure of 6.9 kPa above atmosphere was considered. As expected, a smaller change in pressure produces a much smaller difference between the rise and fall in indicated pressure. The reduced difference is due to minimal nonlinearity in the smaller portion of the Stern–Volmer curve that is traversed by the small pressure jump. The trend remains the same, however: the response to a pressure decrease is faster than the response to a pressure increase.

The effect of the overall range of the pressure change is shown by comparing Fig. 6 with Fig. 9. Both cases have a pressure change of 101 kPa, but the first case is a change to vacuum and back, whereas

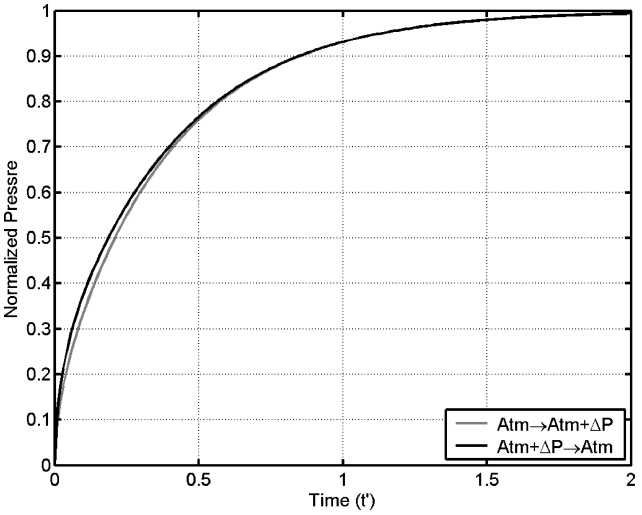

Fig. 8 PSP-indicated pressure step response, variation with pressure-jump magnitude: $A = 0.9$, $B = 0.1$, $\gamma = 1.0$, and $\Delta P = 6.9$ kPa.

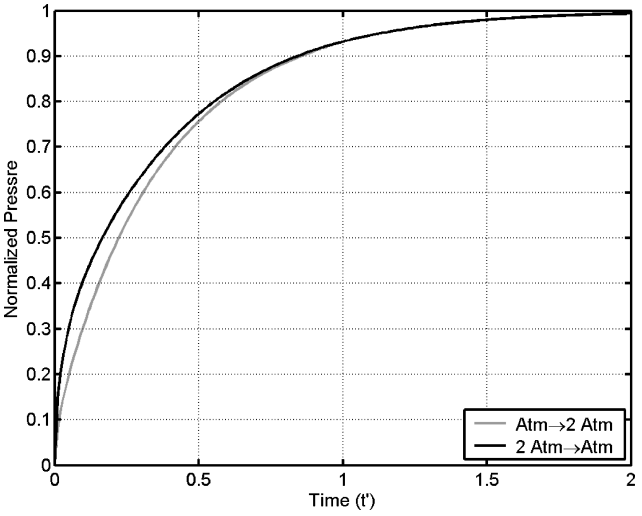

Fig. 9 PSP-indicated pressure step response, variation from 1 to 2 atm: $A = 0.9$, $B = 0.1$, and $\gamma = 1.0$.

the second case is a change from 101 to 202 kPa and back. Note that the pressure change at lower pressures produces a greater difference in the time scales of the indicated pressure than the change at higher pressures. The effect of the mean pressure on the indicated pressure-jump response is due to the nonlinear nature of the Stern–Volmer curve. Figure 4 shows that the highly nonlinear region of the curve is focused at lower pressures, whereas the curve becomes more linear at high pressures.

Frequency Response

The preceding-step-response data were modeled for typical pressure-sensitive paint calibrations. These data provide a foundational understanding of the diffusion and quenching mechanisms responsible for the nonlinear response characteristics. The following results extend the preceding data by incorporating experimental calibration data for two PSP formulations and generalizing the model to allow for an arbitrary input for pressure time-history.

The present solution scheme remains the same as the previous derivation, except that an alternative method is employed for calculating the distribution of gas concentration within the paint layer. The following results are based on the modal analysis technique presented by Winslow et al.[39] The system of equations to be solved for oxygen concentration is given by

$$\begin{pmatrix} \vdots \\ \dot{\alpha}_i(t') \\ \vdots \end{pmatrix} = \begin{bmatrix} \ddots & 0 & 0 \\ 0 & -\lambda_i^2 & 0 \\ 0 & 0 & \ddots \end{bmatrix} \begin{pmatrix} \vdots \\ \alpha_i(t') \\ \vdots \end{pmatrix} + \begin{bmatrix} \vdots & \vdots \\ 0 & -2\sin(\lambda_i)/\lambda_i \\ \vdots & \vdots \end{bmatrix} \begin{pmatrix} P'(t') \\ \dot{P}'(t') \end{pmatrix} \tag{22}$$

$$n(x', t') = \begin{pmatrix} \cdots & \cos(\lambda_i x') & \cdots \end{pmatrix} \begin{pmatrix} \vdots \\ \alpha_i(t') \\ \vdots \end{pmatrix} + \begin{pmatrix} 1 & 0 \end{pmatrix} \begin{pmatrix} P'(t') \\ \dot{P}'(t') \end{pmatrix} \tag{23}$$

where P' is the dimensionless input pressure waveform. Complete details of the derivation of this system of equations are given by Winslow et al.[39] Equations (22) and (23) were modeled with 200 steps through the paint thickness, 500 steps in time, and 100 wave numbers to provide the distribution of oxygen concentration throughout the paint thickness for an arbitrary pressure time-history. The oxygen concentration is then converted to an intensity by a Stern–Volmer intensity calibration for the paint of interest. The intensity is integrated over the paint thickness and then converted back to an indicated pressure by the same Stern–Volmer calibration for the subject paint.

To evaluate the response characteristics of actual paint formulations, Eqs. (22) and (23) are solved for a sine wave over a range of frequencies and experimental calibrations (Figs. 3 and 4) are used in the modeling process. The responses of both fast FIB and polymer/ceramic PSP are evaluated across a range of frequencies, and compared with the response for a linear calibration. Two pressure ranges were considered, from atmosphere to pure oxygen ($[O_2] = 1$) and from atmosphere to pure nitrogen ($[O_2] = 0$), both varying in a sinusoidal fashion. Bode plots for the fast FIB results are shown in Fig. 10. The asymptote for the linear calibration response is -10 dB per decade, and the phase delay levels out at -45 deg. There is a difference in the frequency roll-off characteristics between the nitrogen and oxygen waveforms, however. Notice that the differences in response only become significant when the flowfield frequency has exceeded the frequency response of the paint ($\omega\tau > 1$). Table 1 summarizes the magnitude and phase delay characteristics shown

Table 1 Frequency response characteristics

	Linear calibration		Fast FIB		Polymer/ceramic	
Gas	Magnitude, dB/decade	Phase, deg	Magnitude, dB/decade	Phase, deg	Magnitude, dB/decade	Phase, deg
Nitrogen	−10.0	−45	−9.37	−36	−9.90	−42
Oxygen	−10.0	−45	−9.78	−41	−9.94	−44

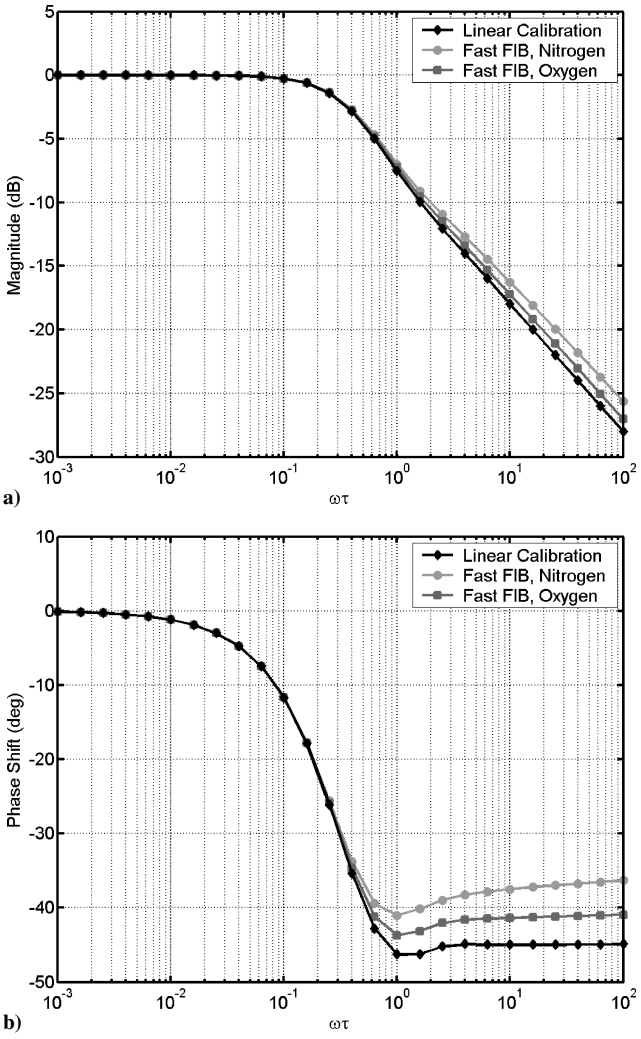

Fig. 10 Bode plots of a) magnitude and b) phase for the frequency response of fast FIB PSP.

in Fig. 10. The magnitude attenuation is defined as

$$\text{Mag} = 20\log_{10}\left(\frac{\text{std}(P_{\text{output}})}{\text{std}(P_{\text{input}})}\right) \tag{24}$$

and the average phase delay is defined as

$$\bar{\phi} = \frac{1}{N}\sum_{i=1}^{N}\left[\arcsin\left(P^i_{\text{output}}\right) - \arcsin\left(P^i_{\text{input}}\right)\right] \tag{25}$$

because the output wave form is distorted through the nonlinear system.

The same flowfield inputs of nitrogen and oxygen sine waves were modeled for the polymer/ceramic paint. Bode plots for these results are shown in Fig. 11. The nitrogen and oxygen responses are very similar and relatively close to the linear calibration roll-off of -10 dB per decade. The plateau in the phase delay also exhibits less variation than in the fast FIB case. The reason for the diminished variation is that the intensity response of the polymer/ceramic paint

Table 2 Summary of dynamic calibration methods

Method	Δt	Δp	References
Shock tube	1 μs	101-kPa increase only	Sakaue and Sullivan,[10] Asai et al.[15]
Solenoid valve	1 ms	101-kPa increase/decrease	Baron et al.,[7] Asai et al.,[8] Teduka et al.,[9] Carroll et al.,[38] Fonov et al.,[49] Asai[50]
Loudspeaker	10 μs	1.2-kPa sinusoidal	Jordan et al.,[51] Boerrigter and Charbonnier[52]
Siren pressure generator	100 μs	60-kPa sinusoidal	Davis and Zasimowich[53]
Pulsating jet	667 μs	250-kPa increase/decrease	Sakamura et al.[54]
Fluidic oscillator	50 μs	101-kPa increase/decrease	Gregory et al.[19,21]

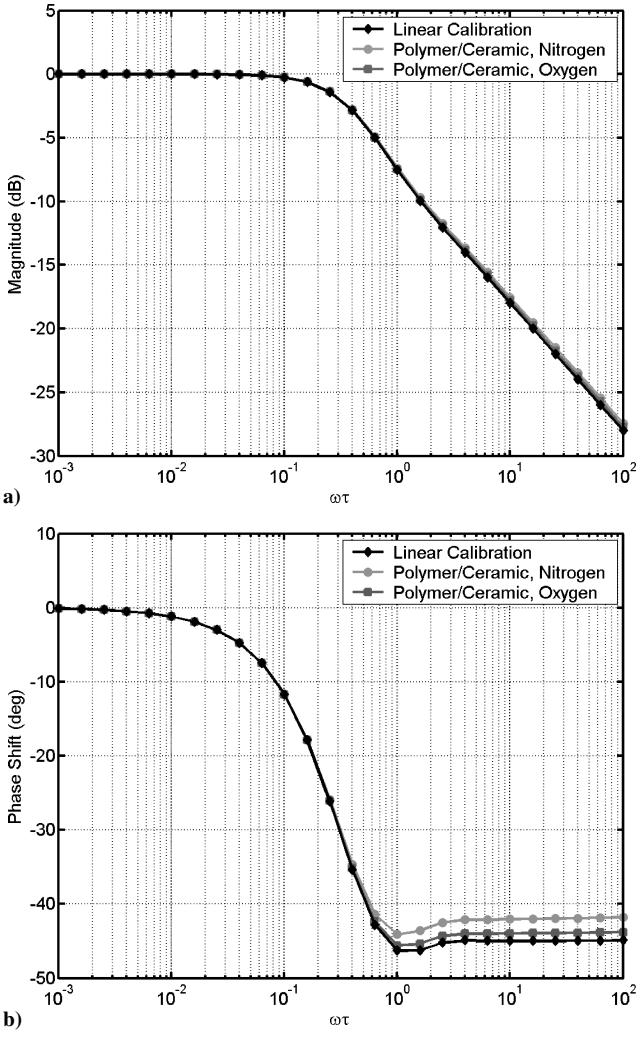

Fig. 11 Bode plots of a) magnitude and b) phase for the frequency response of fast FIB PSP.

calibration is not as strongly nonlinear as the fast FIB calibration, as shown in Fig. 4.

Adsorption Effects

Some researchers have observed hysteresis effects in the paint response during PSP tests in a cryogenic wind tunnel.[43] It has been suggested that this observed hysteresis may be due to adsorption of gases on the porous PSP surface and could have implications on the unsteady response of PSP. If a significant quantity of nitrogen, oxygen, or some other gas adsorbs onto the porous paint surface, then the indicated intensity response of the paint may not be a true representation of the local gas concentration. The luminophore molecules are typically adsorbed on the paint surface (as in the case of anodized aluminum PSP[44]) and thus are primarily responsive to any gas that may be adsorbed on the paint surface. If there are no gas molecules adsorbed on the porous surface, then the luminophore responds primarily to gas collisions. These two quenching mechanisms—adsorption-controlled and collision-controlled—are discussed in more detail by Sakaue.[45]

Porous surfaces such as Zeolite X[46] or anodized alumina surfaces[47] are commonly used in gas separation processes because the rates of adsorption differ between various gas species. The affinity of a given gas species for adsorption on a particular surface is given by the heat of sorption Q. Published values for nitrogen, oxygen, and argon on porous surfaces[46] indicate that heats of sorption for nitrogen are typically 1.5 times the values for oxygen or argon. The length of time that a gas molecule remains in contact with a surface is called the adsorption time. DeBoer[48] gives a relation for the adsorption time as

$$\tau_{\text{ads}} = \tau_0 \exp(Q/RT) \tag{26}$$

where τ_0 is the oscillation time of molecules in the adsorbed state, a constant of about 1.6×10^{-13} s. Thus, the adsorption time increases exponentially with the heat of sorption. Because nitrogen typically has a higher heat of sorption for porous surfaces, the adsorption time will be longer for nitrogen than for oxygen.

In relation to the present study, the primary question is whether this adsorption time is large enough to affect the observed quenching behavior of the PSP. If one assumes ambient conditions (298 K) and an aggressive value for the heat of sorption (28.8 kJ/mol for nitrogen on CaNaX-97; Ref. 46), the adsorption time is still only 18 ns. For the adsorption time to be on the order of 1 ms at ambient conditions, the heat of sorption must be approximately 56 kJ/mol. Now if more conservative values for the heat of sorption (15 kJ/mol) and cryogenic temperature (100 K) are assumed, then the adsorption time is on the order of 10 μs. Thus, adsorption effects may become critical at cryogenic temperatures with porous surfaces. For the present evaluation under ambient conditions, however, adsorption effects are assumed negligible.

Experimental Results

The objective of the following work is to verify the results of the diffusion model experimentally. It is difficult to demonstrate this nonlinear quenching behavior experimentally with fast paints because most dynamic calibration devices are limited by either frequency response or pressure range. Calibration tools that have commonly been used include shock tube facilities,[10,15] solenoid valves,[7,9,38,49,50] loudspeakers,[51,52] siren pressure generators,[53] pulsating jets,[54] and fluidic oscillators.[19,21] The characteristics of these calibration techniques are summarized in Table 2.

These calibration methods have various limitations. Loudspeakers typically have a frequency response on the order of a few hundred kilohertz, but it is difficult to generate pressure waves with large enough amplitude for a useful calibration. Solenoid valves are quite common and can generate a step change in pressure, but are plagued by ringing and a response time that is not fast enough to characterize porous PSP formulations. Shock tube facilities are most common for calibrating transducer response, but can only generate a step increase in pressure. Modulated jets can provide a pressure increase and decrease, but typically are not fast enough to calibrate fast paints.

The ideal calibration tool for demonstrating the quenching kinetics of PSP must have a frequency that is much faster than the expected response of the paint. Ideally, this frequency should be arbitrarily specified and independent of pressure. Furthermore, the ideal calibrator should generate arbitrary pressure ranges, mean pressures,

and pressure jump direction. Such a device is not currently available, but the fluidic oscillator approaches this ideal calibrator.

Fluidic Oscillator

To evaluate the quenching kinetics of porous PSP experimentally, a fluidic oscillator is used. The unsteady flow of the oscillator is suitable for making dynamic measurements. A typical fluidic oscillator design is shown in Fig. 12. In this design, a jet of fluid emerges from an orifice called the power nozzle. The issuing jet will tend to attach to one of the side walls by the Coanda effect. The wall attachment occurs because a region of low pressure between the jet and the wall is generated by the jet flow, pulling the jet toward the wall until it is attached. Now, if flow is injected at one of the control ports, a separation bubble can be formed between the jet and the wall. If enough fluid is injected, the separation bubble grows to the point of jet detachment. The momentum of the jet, along with pressure gradients, causes the jet to swing to the opposite wall. This motion can be accomplished cyclically by introducing a feedback loop from the jet exit back to the control port. Whenever the jet is attached to an adjacent wall, it feeds fluid into the feedback tube and initiates the separation bubble. In this way, self-sustaining oscillations can be established. Miniature fluidic oscillators are capable of sustained oscillations on the order of several kilohertz, without any moving parts. The oscillation frequency depends primarily on the size of the device and the supply pressure for the jet issuing from the power nozzle. Flow visualization of typical jet oscillations are shown in Fig. 13. Note that this fluidic oscillator is not the same type used in the current experiments, but serves to illustrate the basic nature of the oscillatory flow.

The fluidic oscillator used in these experiments is one that produces a square-wave flow pattern. This is the same identical oscillator that has been characterized by Gregory et al.[19] and Raman and Raghu[55] in the past. The flow pattern of the oscillator is bimodal, as shown in the previous work. This device is used to characterize the unsteady response of PSP because it has a very fast rise time, and the entire oscillation cycle is on the order of 629 μs long.

The rise time of the PSP response to the issuing jet can be compared when the oscillator is operated with different test gases. Argon,

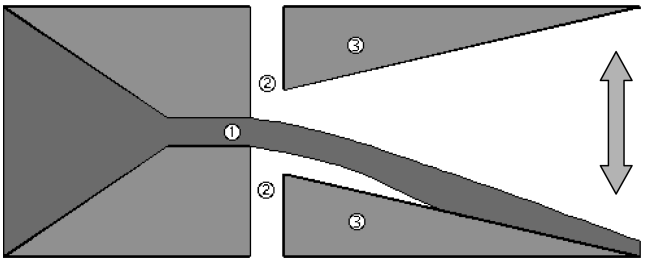

Fig. 12 Fluidic oscillator design demonstrating the operating principle of jet wall attachment: 1, power nozzle; 2, control ports; and 3, attachment walls.

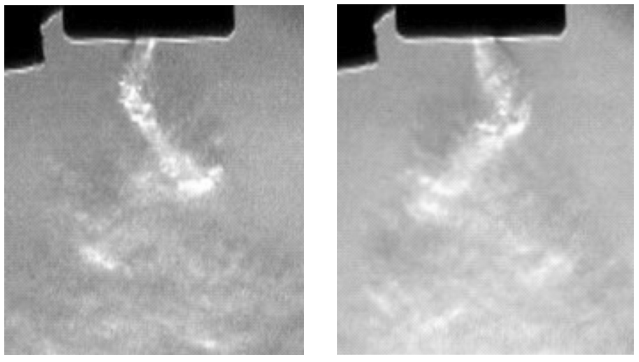

a) **b)**

Fig. 13 Typical schlieren images of fluidic jet oscillations: a) 0- and b) 180-deg phase.

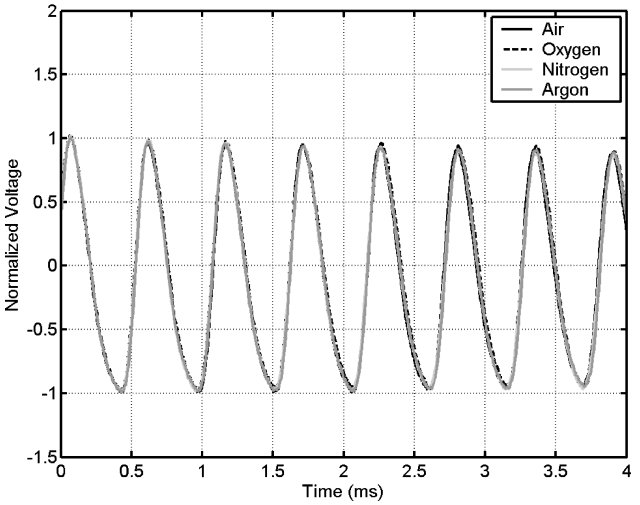

Fig. 14 Hot-film probe characterization of fluidic oscillator flow with various gases. Normalized data indicate no variation.

nitrogen, and oxygen are all used in the current experiments. Argon and nitrogen will both purge the oxygen in the PSP, simulating a pressure decrease to vacuum conditions. The oxygen will have the opposite quenching behavior, with the luminophore being nearly quenched under the presence of pure oxygen. The pure oxygen condition simulates a large pressure increase, up to 482 kPa. If the fluid dynamic behavior of the oscillator is independent of the test gas used, then the PSP response to these three cases may be compared and the response behavior evaluated. Commonality of fluid dynamics among the test gases cannot be immediately assumed, however. Each gas has a different molecular weight and a different speed of sound.[56] Because of this, the supply pressure required of each gas to generate a given oscillation frequency varies somewhat. To evaluate the flow commonality, a hot-film probe was placed in the fluidic oscillator flowfield and subjected to a flow of air, argon, nitrogen, and oxygen. The pressure for each gas was adjusted so that the measured frequency was 1.83 kHz. The normalized time history from each of these gases is shown in Fig. 14. Despite differences in supply pressure, the normalized waveforms have collapsed into one shape. The absence of waveform distortion indicates that the oscillator may be used with different test gases to evaluate the PSP response.

The quenching kinetics of two paint formulations was evaluated: fast FIB and polymer/ceramic PSP. The response time of fast FIB is about 1 ms: on the same order of magnitude as the oscillation period of the fluidic oscillator. On the other hand, the response time of the polymer/ceramic PSP is less than 25 μs, much faster than the characteristic time scale of the fluidic oscillator flowfield. The polymer/ceramic PSP sample was prepared with tris(bathophenanthroline) ruthenium dichloride as the luminophore, whereas the fast FIB sample employed platinum tetra(pentafluorophenyl)porphine. Calibration data for the two paint formulations are shown in Fig. 3. The thicknesses of the paint samples were measured with a profilometer: the polymer/ceramic was 73 μm thick, and the fast FIB was on the order of 1 μm thick (near the uncertainty limit of the profilometer). Polymer/ceramic paint samples are not usually as thick as the subject sample. A thick sample was chosen because the diffusion coefficient of porous paints is known to be very high. The aim of this selection is to offset the high diffusion coefficient with a large thickness-squared term in Eq. (1), such that the response time of the paint will approach the time scale of the flowfield.

The experimental setup for the fluidic oscillator is shown in Fig. 15. The paint samples were mounted parallel to and at the edge of the jet exit. The supply gases were argon, nitrogen, or oxygen: all three were set at a pressure such that the oscillation frequency was maintained constant at 1.59 kHz. The corresponding gauge supply pressures were 40.4 kPa for argon, 26.3 kPa for nitrogen, and 31.0 kPa for oxygen.

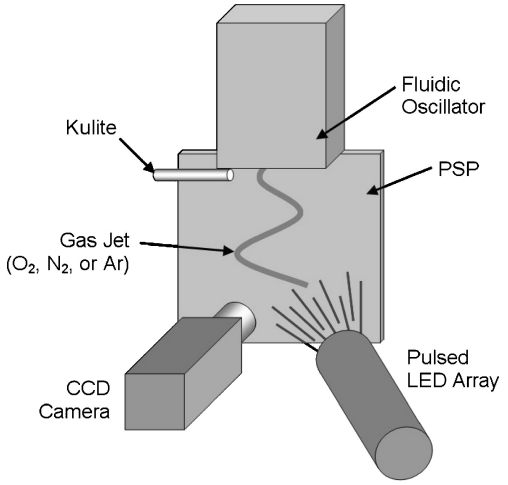

Fig. 15 Experimental setup for fluidic oscillator.

A Kulite pressure transducer was positioned adjacent to the oscillator to provide a reference signal for triggering and phase-locking. The Kulite signal was low-pass filtered at 2 kHz and high-pass filtered at 1 kHz to eliminate all but the primary frequency component. This filtered signal was sent to an oscilloscope with a gating function and trigger output. The pulsed output from the oscilloscope was used to phase lock the light-emitting diode (LED) illumination with the oscillation frequency. Successive delays within the oscillation period were set with a pulse/delay generator. The pulse width was set to 15.723 μs (2.5% of the oscillation period), and the successive delays were set at 31.446-μs intervals for 20 equal steps throughout the cycle.

A 14-bit charge-coupled device (CCD) camera was used with an f/2.8 macro lens for imaging. An Innovative Scientific Solutions, Inc., blue LED array (465 nm) was used for excitation of the polymer/ceramic PSP, and a violet LED array (405 nm) was used for the fast FIB PSP. A long-pass colored glass filter (590 nm) eliminated the excitation light from the image, leaving only the paint luminescence. The camera shutter was set open for a long period to integrate enough light, whereas the LED array was strobed to freeze and phase-average the oscillatory motion. The exposure time for the polymer/ceramic paint was 60 ms because it is a very bright paint, whereas the fast FIB paint required an exposure time of 2.5 s.

Acquired intensity images were converted to gas concentration levels through a priori paint calibrations (Fig. 3). Each paint sample was calibrated from vacuum up to 100% oxygen at atmospheric pressure. This calibration range corresponds to a variation in pressure from vacuum to 482 kPa. In the data reduction process, an intensity ratio of a wind-off and wind-on image was computed. To eliminate any bias error due to temporal light variation, the intensity ratio was normalized by a point on the PSP known to be under atmospheric conditions. Finally, the intensity ratio was spatially filtered with a 3-pixel square window.

In the current PSP tests, any experimental errors are predominantly due to random shot noise on the CCD array and bias errors in the a priori calibration. Errors due to the temperature sensitivity of PSP are considered negligible, and any cooling due to the jet flow is the same for all three test gases. Random shot noise error is estimated to be $\pm 0.2\%$, and all bias errors are estimated to be $\pm 3\%$.

Results

Typical full-field PSP images of the fluidic oscillator, in response to argon gas, are shown in Fig. 16 for polymer/ceramic PSP. Corresponding results for the paint response to oxygen gas are shown in Fig. 17. Full-field results for the nitrogen gas are fairly identical to the argon data, because both gases purge away oxygen and cause the paint luminescence to increase. The nitrogen and argon jets thus simulate a decrease in pressure down to a vacuum (a change in 101 kPa). The oxygen jet, on the other hand, serves to quench the paint luminescence and simulates a change in pressure from atmospheric conditions up to 482 kPa for 100% oxygen.

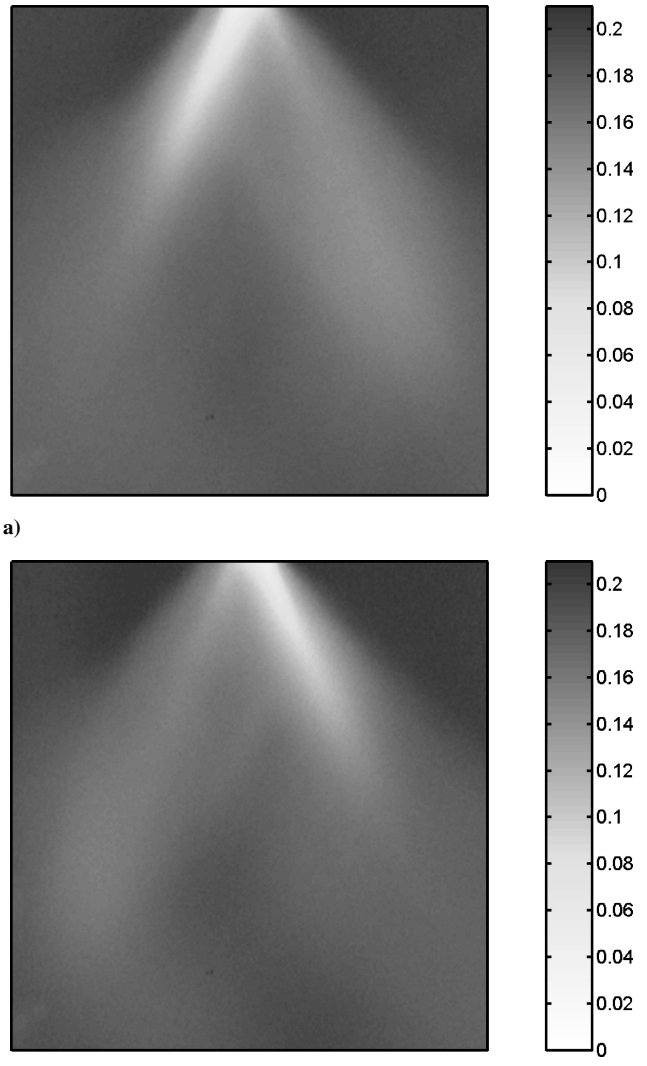

Fig. 16 Polymer/ceramic PSP response to the argon jet at a) 0 μs and b) 314 μs (180-deg delay) at an oscillation frequency of 1.59 kHz.

The data shown in Figs. 16 and 17 represent an oscillation frequency of 1.59 kHz (629-μs period) at a supply pressure of 40.4 kPa for argon and 31.0 kPa for oxygen. Notice that the jet switches between left and right extrema in the oscillation process. This particular oscillator generates a square waveform, with the jet pulsing between the left and right outputs. These PSP measurements compare well with the water visualization performed by Raman and Raghu[55] on the exact same oscillator. The distributions of gas concentration for the two cases are very similar. The primary difference is the scaling of the data: the argon jet purges oxygen and sends the value toward zero, but the oxygen jet increases the value toward unity.

A wealth of information is available from the PSP measurements since the data are phase-locked with images taken throughout the oscillation period. Each pixel location in the data set represents an individual phase-averaged time history of the paint response. This array of time histories throughout the fluidic oscillator flowfield may be compared between the three test gases. To verify the diffusion-based model for these fast paints, the time history at the same point in the flowfield is examined for all three gases. If there is no difference between the time histories for each gas, then either the paint is so fast that quenching kinetics are negligible, or the diffusion model is insufficient. If, on the other hand, there is a difference in response between the gases, then the effects of the modeled response may be evaluated. Recall that the diffusion model predicts that the response of PSP to a step decrease in pressure will be faster than the step

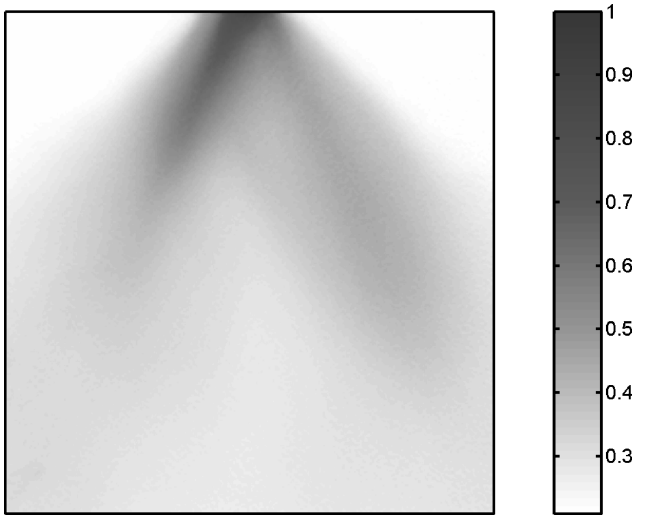

a)

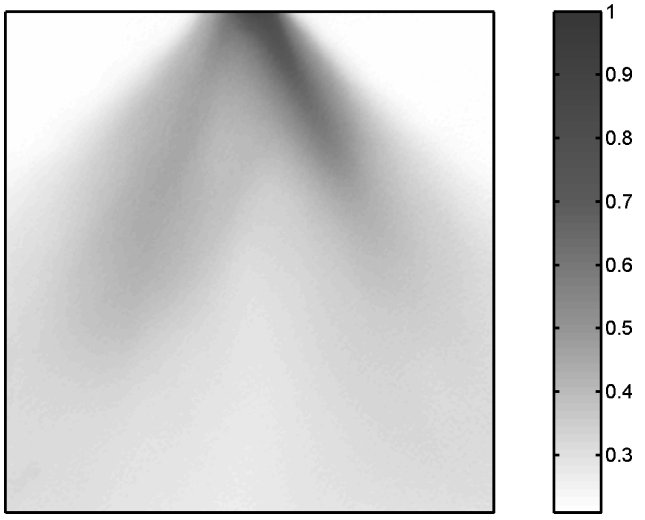

b)

Fig. 17 Polymer/ceramic PSP response to the oxygen jet at a) 0 μs and b) 314 μs (180-deg delay) at an oscillation frequency of 1.59 kHz.

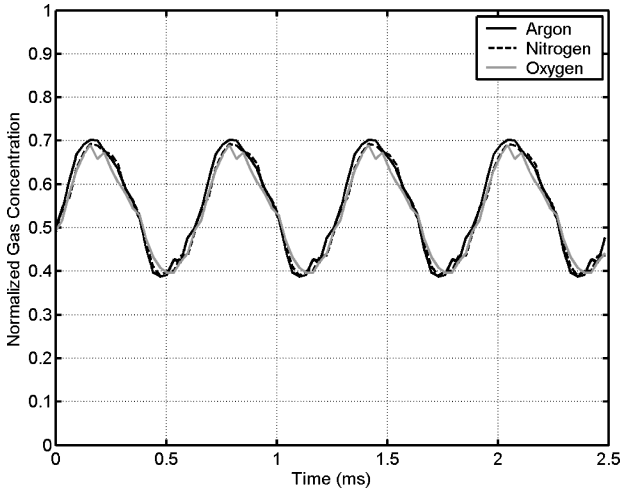

Fig. 18 Polymer/ceramic PSP response to argon, nitrogen, and oxygen jets from the fluidic oscillator at 1.59 kHz.

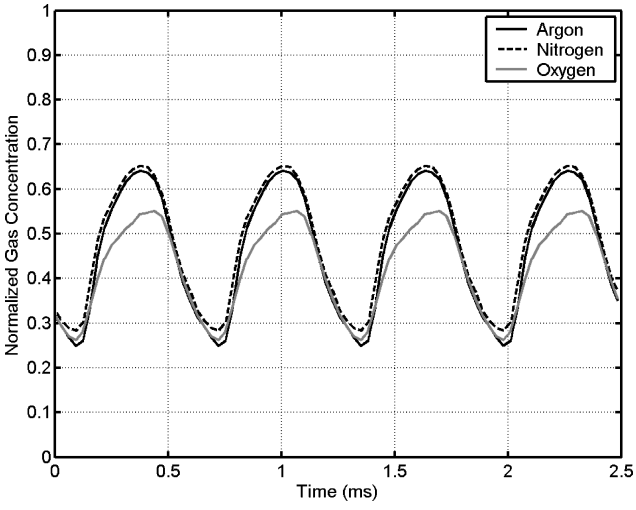

Fig. 19 Fast FIB response to argon, nitrogen, and oxygen jets from the fluidic oscillator at 1.59 kHz.

increase response. If the diffusion model is applicable to these tests, then the PSP response to nitrogen or argon is expected to be faster than the oxygen response.

Comparisons of the polymer/ceramic PSP response to argon, nitrogen, and oxygen are shown in Fig. 18. These compiled time histories are phase-averaged and the gas-concentration amplitude is normalized to a scale from 0 to 1. Unity represents complete gas saturation, while zero represents atmospheric conditions. Within the experimental uncertainty, polymer/ceramic exhibits no phase delay and no magnitude differences between the responses to the argon, nitrogen, or oxygen jets. This indicates that the polymer/ceramic formulation is able to respond to pressure fluctuations at 1.59 kHz and a range of about 5 atm with no frequency delay. This is noteworthy, considering that the thickness of the paint sample is so high (73 μm). These data indicate that the response time of the polymer/ceramic paint is faster than 629 μs and that the diffusion coefficient is greater than 8.4×10^6 μm^2/s.

Data for the response of fast FIB paint to each of the gases are shown in Fig. 19. The measurement location is not in the same position in the flowfield as the polymer/ceramic data in Fig. 18, so the amplitudes of the two data sets do not necessarily correlate. Note that the argon and nitrogen time histories in Fig. 19 correlate well with one another, despite the difference in supply pressures. The response to the oxygen jet, however, never reaches the full magnitude that the nitrogen or argon jets achieve. Furthermore, the oxygen rise time is delayed relative to the argon and nitrogen responses, but exhibits a faster decay time. These properties indicate that the PSP response to the oxygen jet is quite slow relative to the argon or nitrogen jet responses. This behavior agrees quite well with the predicted response from the diffusion model. Even though the fast FIB is an extremely thin layer, it is not suitable for tests in this extreme frequency and pressure range. The fast FIB formulation may be entirely suitable for tests at slightly lower frequency and with smaller pressure changes. This highlights the importance of evaluating not only the thickness and diffusivity characteristics of the paint, but also the expected pressure ranges that will be measured when estimating the suitability of a paint formulation for a particular test.

A quantitative comparison between the model predictions and the fast FIB experimental results is shown in Fig. 20. Here the input to the diffusion model is the hot-film probe data shown in Fig. 14, with the amplitude being arbitrarily scaled to provide the best fit. The predicted response from the diffusion model compares quite well with the measured experimental results for the nitrogen and oxygen jets. The value of the diffusion coefficient was varied until the best fit was achieved between the model and the experimental results, giving a value of 633 μm^2/s. The rms error for this fit is 1.6% gas concentration for the nitrogen jet and 1.1% gas concentration for the nitrogen get. The value of diffusion coefficient measured by these experiments compares well with the quoted values of Winslow et al.[39] (660 μm^2/s) for a polymer-based binder with ruthenium and the estimated values of Drouillard and Linne[40] (300–1000 μm^2/s)

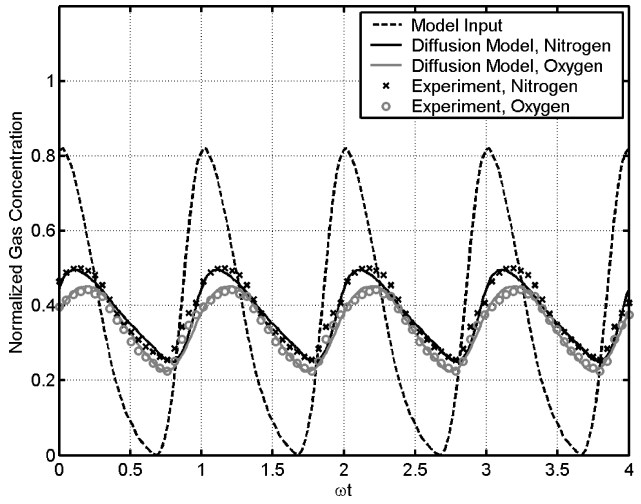

Fig. 20 Comparison of diffusion model with experimental results for nitrogen and oxygen jets.

for Uni-FIB paint. Because the thickness of the subject fast FIB paint sample is approximately 1 μm, Eq. (1) yields a time constant for the paint sample of 1.6 ms. These experimental data fall at the point $\omega\tau = 10^{0.4}$ on the Bode plot in Fig. 10.

Conclusions

This work has shown through modeling and experiments that the unsteady response of PSP is affected by the nonlinear nature of the Stern–Volmer calibration. A calibration that is highly nonlinear will cause the paint to respond quickly to a decrease in oxygen concentration (pressure decrease) and relatively slowly to oxygen sorption (pressure increase). In addition, it has been shown that this observed affect is more pronounced for larger changes in pressure, particularly if the pressure change covers the nonlinear portion of the Stern–Volmer curve at low pressures. The effect of the Freundlich isotherm on the Stern–Volmer relationship produced a minimal variation from the quenching effects of the basic Stern–Volmer relation. Ultimately, it was found that these nonlinear effects only become significant when the characteristic time scale of the flowfield is faster than the response time of the paint.

The unsteady flowfield of a fluidic oscillator was used to verify the model predictions and evaluate the response characteristics of two paint formulations. Experimental results with polymer/ceramic PSP demonstrated no frequency roll-off at 1.59 kHz, indicating that the diffusion coefficient is at least 8.4×10^6 μm^2/s. Results with the fast FIB paint formulation did demonstrate the nonlinear response characteristics predicted by the diffusion model. The fast FIB results indicated a much slower response to an increase in oxygen when compared to argon or nitrogen at the same conditions. A quantitative comparison between the fast FIB results and the diffusion model showed good agreement and yielded a diffusion coefficient of 633 μm^2/s and a time constant of 1.6 ms for the 1-μm-thick fast FIB paint.

Acknowledgments

This work was funded by the NASA Graduate Student Researchers Program under the guidance of Tim Bencic at NASA John H. Glenn Research Center at Lewis Field. The Boeing Company lent a 14-bit CCD camera for these experiments, and their help is appreciated. Jim Crafton of Innovative Scientific Solutions, Inc., provided the fast FIB paint sample evaluated in these experiments. Surya Raghu of Advanced Fluidics Corp. provided the fluidic oscillator used in these tests.

References

[1]Peterson, J. I., and Fitzgerald, R. V., "New Technique of Surface Flow Visualization Based on Oxygen Quenching of Fluorescence," *Review of Scientific Instruments*, Vol. 51, No. 5, 1980, pp. 670, 671.

[2]Kavandi, J., Callis, J., Gouterman, M., Khalil, G., Wright, D., Green, E., Burns, D., and McLachlan, B., "Luminescent Barometry in Wind Tunnels," *Review of Scientific Instruments*, Vol. 61, No. 11, 1990, pp. 3340–3347.

[3]McLachlan, B. G., Kavandi, J. L., Callis, J. B., Gouterman, M., Green, E., Khalil, G., and Burns, D., "Surface Pressure Field-Mapping Using Luminescent Coatings," *Experiments in Fluids*, Vol. 14, Nos. 1–2, 1993, pp. 33–41.

[4]Bell, J. H., Schairer, E. T., Hand, L. A., and Mehta, R. D., "Surface Pressure Measurements Using Luminescent Coatings," *Annual Review of Fluid Mechanics*, Vol. 33, 2001, pp. 155–206.

[5]Liu, T., Campbell, B. T., Burns, S. P., and Sullivan, J. P., "Temperature- and Pressure-Sensitive Luminescent Paints in Aerodynamics," *Applied Mechanics Reviews*, Vol. 50, No. 4, 1997, pp. 227–246.

[6]Liu, T., and Sullivan, J. P., *Pressure and Temperature Sensitive Paints*, Springer, New York, 2005, pp. 175–178.

[7]Baron, A. E., Danielson, J. D. S., Gouterman, M., Wan, J. R., Callis, J. B., and McLachlan, B., "Submillisecond Response Times of Oxygen-Quenched Luminescent Coatings," *Review of Scientific Instruments*, Vol. 64, No. 12, 1993, pp. 3394–3402.

[8]Asai, K., Kanda, H., Cunningham, C. T., Erausquin, R., and Sullivan, J. P., "Surface Pressure Measurements in a Cryogenic Wind Tunnel by Using Luminescent Coatings," *ICIASF 1997 Record, 17th International Congress on Instrumentation in Aerospace Simulation Facilities*, Inst. of Electrical and Electronics Engineers, Piscataway, NJ, 1997, pp. 105–114.

[9]Teduka, N., Kameda, M., Asai, K., Amao, Y., and Nakakita, K., "Adsorptive Pressure-Sensitive Coatings for Unsteady Flow Measurements," *Transactions of the Japan Society of Mechanical Engineers, Part B*, Vol. 68, No. 669, 2002, pp. 1391–1399 (in Japanese).

[10]Sakaue, H., and Sullivan, J. P., "Time Response of Anodized Aluminum Pressure-Sensitive Paint," *AIAA Journal*, Vol. 39, No. 10, 2001, pp. 1944–1949.

[11]Sakaue, H., Sullivan, J. P., Asai, K., Iijima, Y., and Kunimasu, T., "Anodized Aluminum Pressure Sensitive Paint in a Cryogenic Wind Tunnel," *Instrumentation in the Aerospace Industry: Proceedings of the International Symposium*, Instrument Society of America, Albuquerque, NM, 1999, pp. 337–346.

[12]Scroggin, A. M., Slamovich, E. B., Crafton, J. W., Lachendro, N., and Sullivan, J. P., "Porous Polymer/Ceramic Composites for Luminescence-Based Temperature and Pressure Measurement," *Materials Research Society Symposium—Proceedings*, Vol. 560, Materials Research Society, Warrendale, PA, 1999, pp. 347–352.

[13]Scroggin, A. M., "Processing and Optimization of Doped Polymer/Ceramic Composite Films for Luminescence-Based Pressure and Temperature Measurement in Aerodynamic Applications," M.S. Thesis, School of Materials Engineering, Purdue Univ., West Lafayette, IN, Dec. 1999.

[14]Masuda, T., Isobe, E., Higashimura, T., and Takada, K., "Poly[1-(Trimethylsilyl)-1-Propyne]—A New High Polymer Synthesized with Transition-Metal Catalysts and Characterized by Extremely High Gas-Permeability," *Journal of the American Chemical Society*, Vol. 105, No. 25, 1983, pp. 7473–7474.

[15]Asai, K., Nakakita, K., Kameda, M., and Teduka, K., "Recent Topics in Fast-Responding Pressure-Sensitive Paint Technology at National Aerospace Laboratory," *ICIASF 2001 Record, 19th International Congress on Instrumentation in Aerospace Simulation Facilities*, Inst. of Electrical and Electronics Engineers, Piscataway, NJ, 2001, pp. 25–36.

[16]Asai, K., Amao, Y., Iijima, Y., Okura, I., and Nishide, H., "Novel Pressure-Sensitive Paint for Cryogenic and Unsteady Wind-Tunnel Testing," *Journal of Thermophysics and Heat Transfer*, Vol. 16, No. 1, 2002, pp. 109–115.

[17]Puklin, E., Carlson, B., Gouin, S., Costin, C., Green, E., Ponomarev, S., Tanji, H., and Gouterman, M., "Ideality of Pressure-Sensitive Paint. I. Platinum tetra(pentafluorophenyl)porphine in Fluoroacrylic Polymer," *Journal of Applied Polymer Science*, Vol. 77, No. 13, 2000, pp. 2795–2804.

[18]Sakaue, H., Gregory, J. W., Sullivan, J. P., and Raghu, S., "Porous Pressure-Sensitive Paint for Characterizing Unsteady Flowfields," *AIAA Journal*, Vol. 40, No. 6, 2002, pp. 1094–1098.

[19]Gregory, J. W., Sakaue, H., and Sullivan, J. P., "Fluidic Oscillator as a Dynamic Calibration Tool," AIAA Paper 2002-2701, June 2002.

[20]Kameda, M., Tezuka, N., Hangai, T., Asai, K., Nakakita, K., and Amao, Y., "Adsorptive Pressure-Sensitive Coatings on Porous Anodized Aluminium," *Measurement Science and Technology*, Vol. 15, No. 3, 2004, pp. 489–500.

[21]Gregory, J. W., Sullivan, J. P., Raman, G., and Raghu, S., "Characterization of a Micro Fluidic Oscillator for Flow Control," AIAA Paper 2004-2692, June 2004.

[22]Gregory, J. W., "Unsteady Pressure Measurements in a Turbocharger Compressor Using Porous Pressure-Sensitive Paint," M.S. Thesis, School of Aeronautics and Astronautics, Purdue Univ., West Lafayette, IN, Dec. 2002.

[23]Gregory, J. W., "Porous Pressure-Sensitive Paint for Measurement of Unsteady Pressures in Turbomachinery," AIAA Paper 2004-0294, Jan. 2004.

[24]Gregory, J. W., and Sullivan, J. P., "Characterization of Hartmann Tube Flow with Porous Pressure-Sensitive Paint," AIAA Paper 2003-3713, June 2003.

[25]MacCallum, J. R., and Rudkin, A. L., "Novel Technique for Measuring the Diffusion Constant of Oxygen in Polymer-Films," *European Polymer Journal*, Vol. 14, No. 9, 1978, pp. 655, 656.

[26]Cox, M. E., and Dunn, B., "Oxygen Diffusion in Poly(Dimethyl Siloxane) Using Fluorescence Quenching. 1. Measurement Technique and Analysis," *Journal of Polymer Science Part A. Polymer Chemistry*, Vol. 24, No. 4, 1986, pp. 621–636.

[27]Carraway, E. R., Demas, J. N., and DeGraff, B. A., "Photophysics and Oxygen Quenching of Transition-Metal Complexes on Fumed Silica," *Langmuir*, Vol. 7, No. 12, 1991, pp. 2991–2998.

[28]Mills, A., and Chang, Q., "Modeled Diffusion-Controlled Response and Recovery Behavior of a Naked Optical Film Sensor with a Hyperbolic-Type Response to Analyte Concentration," *Analyst*, Vol. 117, No. 9, 1992, pp. 1461–1466.

[29]Yekta, A., Masoumi, Z., and Winnik, M. A., "Luminescence Measurements of Oxygen Permeation and Oxygen Diffusion in Thin Polymer Films," *Canadian Journal of Chemistry—Revue Canadienne de Chimie*, Vol. 73, No. 11, 1995, pp. 2021–2029.

[30]Masoumi, Z., Stoeva, V., Yekta, A., Pang, Z., Manners, I., and Winnik, M. A., "Luminescence Quenching Method for Probing the Diffusivity of Molecular Oxygen in Highly Permeable Media," *Chemical Physics Letters*, Vol. 261, Nos. 4–5, 1996, pp. 551–557.

[31]Vasil'ev, V. V., and Borisov, S. M., "Optical Oxygen Sensors Based on Phosphorescent Water-Soluble Platinum Metals Porphyrins Immobilized in Perfluorinated Ion-Exchange Membrane," *Sensors and Actuators B, Chemical*, Vol. 82, Nos. 2–3, 2002, pp. 272–276.

[32]Ruffolo, R., Evans, C. E. B., Liu, X. H., Ni, Y. Z., Pang, Z., Park, P., McWilliams, A. R., Gu, X. J., Lu, X., Yekta, A., Winnik, M. A., and Manners, I., "Phosphorescent Oxygen Sensors Utilizing Sulfur–Nitrogen–Phosphorus Polymer Matrixes: Synthesis, Characterization, and Evaluation of Poly(thionylphosphazene)–b–Poly(tetrahydrofuran) Block Copolymers," *Analytical Chemistry*, Vol. 72, No. 8, 2000, pp. 1894–1904.

[33]Lu, X., and Winnik, M. A., "Luminescence Quenching in Polymer/Filler Nanocomposite Films Used in Oxygen Sensors," *Chemistry of Materials*, Vol. 13, No. 10, 2001, pp. 3449–3463.

[34]Jayarajah, C. N., Yekta, A., Manners, I., and Winnik, M. A., "Oxygen Diffusion and Permeability in Alkylaminothionylphosphazene Films Intended for Phosphorescence Barometry Applications," *Macromolecules*, Vol. 33, No. 15, 2000, pp. 5693–5701.

[35]Kneas, K. A., Demas, J. N., Nguyen, B., Lockhart, A., Xu, W. Y., and DeGraff, B. A., "Method for Measuring Oxygen Diffusion Coefficients of Polymer Films by Luminescence Quenching," *Analytical Chemistry*, Vol. 74, No. 5, 2002, pp. 1111–1118.

[36]Liu, T., Teduka, N., Kameda, M., and Asai, K., "Diffusion Timescale of Porous Pressure-Sensitive Paint," *AIAA Journal*, Vol. 39, No. 12, 2001, pp. 2400–2402.

[37]Schairer, E. T., "Optimum Thickness of Pressure-Sensitive Paint for Unsteady Measurements," *AIAA Journal*, Vol. 40, No. 11, 2002, pp. 2312–2318.

[38]Carroll, B. F., Abbitt, J. D., Lukas, E. W., and Morris, M. J., "Step Response of Pressure-Sensitive Paints," *AIAA Journal*, Vol. 34, No. 3, 1996, pp. 521–526.

[39]Winslow, N. A., Carroll, B. F., and Kurdila, A. J., "Model Development and Analysis of the Dynamics of Pressure-Sensitive Paints," *AIAA Journal*, Vol. 39, No. 4, 2001, pp. 660–666.

[40]Drouillard, T. F., II, and Linne, M. A., "Luminescence Lifetime Response of Pressure-Sensitive Paint to a Pressure Transient," *AIAA Journal*, Vol. 43, No. 5, 2005, pp. 1100–1108.

[41]Bird, R. B., Stewart, W. E., and Lightfoot, E. N., "Diffusivity and the Mechanisms of Mass Transport," *Transport Phenomena*, Wiley, New York, 1960, Chap. 16.

[42]Stern, O., and Volmer, M., "Uber die Abklingungszeit der Fluoreszenz," *Physikalische Zeitschrift*, Vol. 20, No. 8, 1919, pp. 183–188.

[43]Egami, Y., Iijima, Y., and Asai, K., "Hysteresis of Pressure-Sensitive Paint in Cryogenic Wind Tunnels," *Proceedings of the 34th Fluid Dynamics Conference*, Kochi Univ., Kochi, Japan, 2002 (in Japanese).

[44]Teduka, N., Kameda, M., Asai, K., Amao, Y., and Nakakita, K., "Adsorptive Pressure-Sensitive Coatings for Unsteady Flow Measurements," *Transactions of the Japan Society of Mechanical Engineers. Series B*, Vol. 68, No. 669, 2002, pp. 1391–1399.

[45]Sakaue, Hirotaka, "Porous Pressure Sensitive Paints for Aerodynamic Applications," M.S. Thesis, School of Aeronautics and Astronautics, Purdue Univ., West Lafayette, IN, Dec. 1999.

[46]Jasra, R. V., Choudary, N. V., and Bhat, S. G. T., "Correlation of Sorption Behavior of Nitrogen, Oxygen, and Argon with Cation Locations in Zeolite X," *Industrial and Engineering Chemistry Research*, Vol. 35, No. 11, 1996, pp. 4221–4229.

[47]Crawford, G. P., Steele, L. M., Ondris-Crawford, R., Iannacchione, G. S., Yeager, C. J., Doane, J. W., and Finotello, D., "Characterization of the Cylindrical Cavities of Anapore and Nuclepore Membranes," *Journal of Chemical Physics*, Vol. 96, No. 10, 1992, pp. 7788–7796.

[48]DeBoer, J. H., *The Dynamical Character of Adsorption*, 2nd ed., Clarendon, Oxford, 1968, pp. 30–32.

[49]Fonov, S. D., Engler, R. H., Klein, C., Mihailov, S. V., Mosharov, V. E., Kulesh, V. P., Radchenko, V. N., and Schairer, E., "Pressure Sensitive Paint for Oscillating Pressure Fields Measurements," *ICIASF '99 Record: 18th International Conference on Instrumentation in Aerospace Simulation Facilities*, Inst. of Electrical and Electronics Engineers, Piscataway, NJ, 1999, pp. 24–1.

[50]Asai, K., "Status of Pressure Sensitive Paint Technology at National Aerospace Laboratory," *ICIASF 1999 Record, 18th International Congress on Instrumentation in Aerospace Simulation Facilities*, Inst. of Electrical and Electronics Engineers, Piscataway, NJ, 1999, pp. 15.1–15.11.

[51]Jordan, J. D., Weaver, W. L., Trump, D. D., Sarka, B., Goss, L. P., Navarra, K. R., and Neal Watkins, A., "Extending PSP Technology for the Investigation of HCF-Related Phenomena," *Instrumentation in the Aerospace Industry: Proceedings of the International Symposium*, Instrument Society of America, Albuquerque, NM, 1999, pp. 327–336.

[52]Boerrigter, H. L., and Charbonnier, J. M., "Design and Calibration of an Unsteady Pressure Measurement System," *ICIASF'97 Record. International Congress on Instrumentation in Aerospace Simulation Facilities*, Inst. of Electrical and Electronics Engineers, Piscataway, NJ, 1997, pp. 185–194.

[53]Davis, P. A. and Zasimowich, R. F., "High Frequency Dynamic Pressure Calibration Technique," *Instrumentation in the Aerospace Industry: Proceedings of the 31st International Instrumentation Symposium*, Instrumentation, Systems, and Automation Society, Research Triangle Park, NC, 1985, pp. 59–91.

[54]Sakamura, Y., Suzuki, T., Matsumoto, M., Masuya, G., and Ikeda, Y., "Optical Measurements of High-Frequency Pressure Fluctuations Using a Pressure-Sensitive Paint and Cassegrain Optics," *Measurement Science and Technology*, Vol. 13, No. 10, 2002, pp. 1591–1598.

[55]Raman, G., and Raghu, S., "Cavity Resonance Suppression Using Miniature Fluidic Oscillators," *AIAA Journal*, Vol. 42, No. 12, 2004, pp. 2608–2612.

[56]John, J. E. A., *Gas Dynamics*, 2nd ed., Prentice–Hall, Englewood Cliffs, NJ, 1984, p. 416.

K. Fujii
Associate Editor